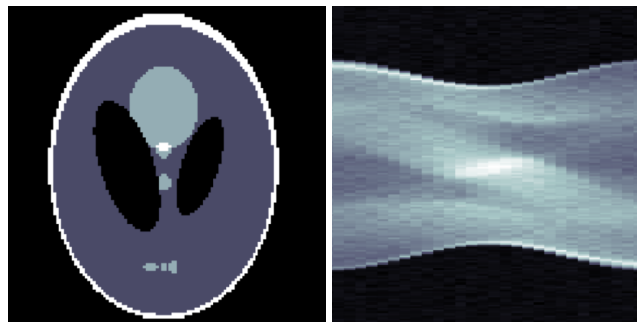

ECE 228 - Milestone Report - Team 22

Chris Light **Michael Ingerman**
UCSD - ECE UCSD - MAE
cdlight@ucsd.edu mingerman@ucsd.edu

1 Introduction

Computed Tomography is one of the most prevalent forms of medical imaging available. Albeit invaluable to doctors in medical decision making, CT scanning still holds a risk to patients as the use of harmful X-ray radiation poses health concerns. There is a delicate balance of not exposing the patient with too much radiation while still producing a meaningful picture. Traditional signal processing methods in CT imaging is bounded by the Nyquist rate, which is a lower limit to the number of projection angles necessary to perform image construction. Reducing the number of angles necessary for a meaningful image means less radiation exposure - and a necessity to break the Nyquist criteria by use of a Deep Neural Network.

In this paper we adapt a method called Deep Back Projection [1] for the purposes of reconstructing CT chest images of Covid19 patients using sparse imaging with a deep convolution neural network (CNN) framework. The advantages of using a CNN is that it reduces the number of parameters of deep neural network by imposing spatial invariance on image data. Using the Harvard's "COVID19-CT-Dataset"[2] we first process each CT image by producing a set of back projected sinogram slices to form a stack of images of parallel lines at different orientations. We then feed this stack as input into our model during training in an attempt to employ learning to compute a fully reconstructed sinogram.



(a) Shepp-Logan phantom

(b) Shepp-Logan sinogram

Figure 1: Left image is a Shepp-Logan Phantom. Right image is a Corresponding sinogram.

2 Background

The Radon transform function computes the projections of an image matrix along a specified direction. For a 2D image, the projections of the image data found via radon transform can be considered a set of line integrals of pixel intensities along parallel paths as can be seen in fig. 2. By sampling axes at various orientations, a set of random transforms can be combined to form a sinogram image like in fig 1. Furthermore, for each orientation of sinogram projection computed via radon transform, the signal intensities for each projection can be cast as parallel lines of uniform intensities along the direction

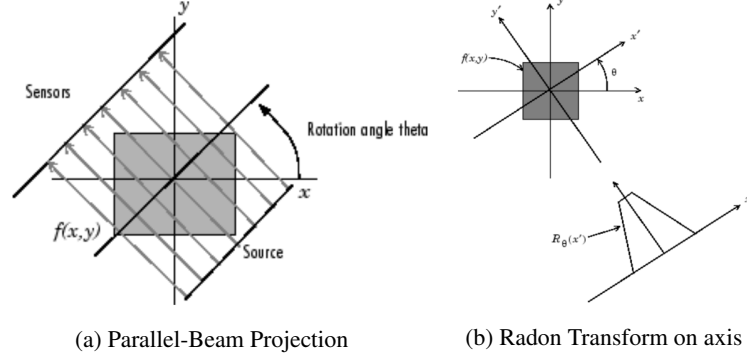


Figure 2: Left image showcases how parallel signals are sent at a given orientation of a source. Right image shows how signals are interpreted through Radon Transform to yield the integral intensities of a signals along an axis.

25 of the original signal as can be seen in fig. 3. The resulting images with parallel lines of uniform
 26 intensities are called back-projected slice sinogram images. Collectively, these back-projected images
 27 are useful since they represent spatial-based information in a non-spatially dependent way. This
 28 makes back-project images a convenient input for a convolution neural network style model.

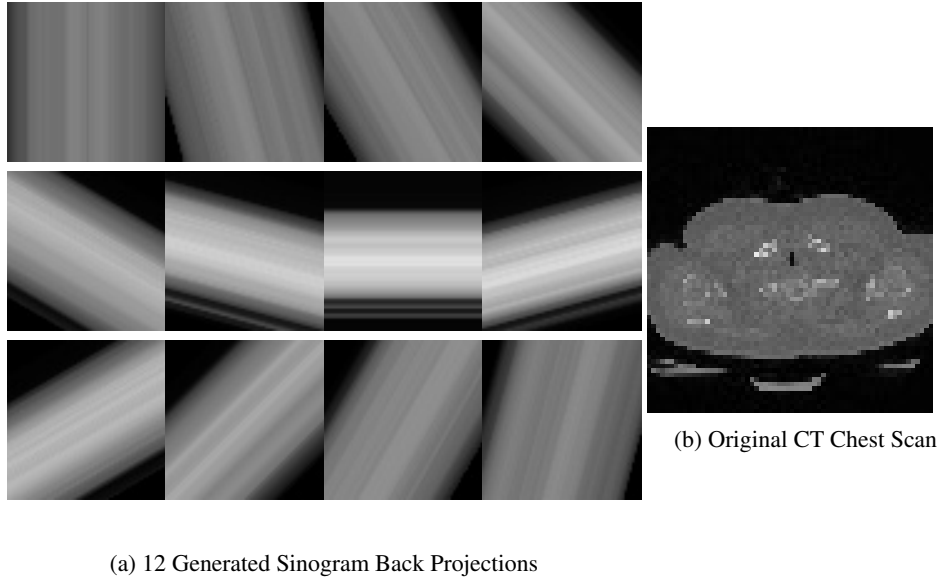


Figure 3: Radon transform is applied to a CT chest scan(truth image) using 12 angles to create a CT sinogram with fixed step size between $0^\circ - 180^\circ$. Single-view back projections are stacked to form the input for the convolution neural network.

29 3 Dataset and Framework

30 3.1 Dataset Processing

31 Truth images for our model were gathered from Harvard's "COVID19-CT-Dataset"[2]. Each truth
 32 image was converted to a set of sinogram projections at different orientations θ_i . Every set of
 33 sinogram projection images y_i was found by first computing a sinogram y from a given truth image
 34 with a set of n angles. The number of slices n corresponding to the range of angles was variably
 35 selected in order to gauge how the model preformed as a function of data sparsity. Then each set
 36 of sinogram projection $y_i \in R^n$ were generated by extracting projections along the set of angles
 37 $\theta_i \in R^n$ for a given sinogram image y .

38 All datasets used to obtain current results contained 568 truth images with 568×12 sinogram slice
 39 projections. Future model training will be done with a dataset of 200,000 truth images and a variable
 40 number of slice projections. No image preprocessing was applied to truth images in our initial
 41 attempts with the exception of image downsizing 128×128 pixels from the original truth image
 42 size of 512×512 pixels. The rationale for doing so was to observe how well our model dealt with
 43 minimally preprocessed data.

44 3.2 Framework Architecture

45 Following the work of [3], we construct a similar architecture to what is seen in fig. 4

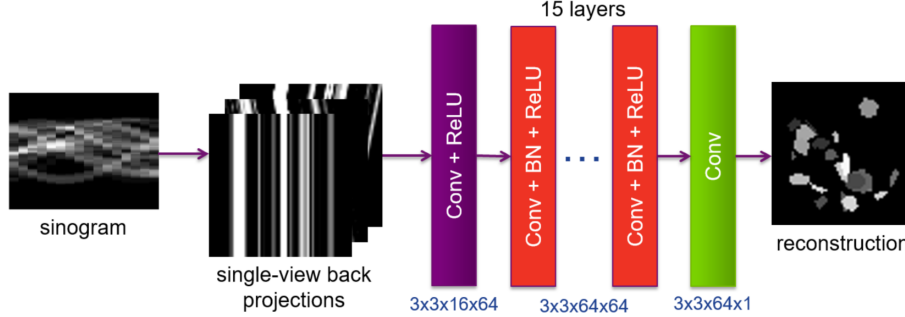


Figure 4: Network Architecture

46 From the dataloader, a torch tensor of size $[b, n+1, h, w]$ is fed into the network; For b = batch size, n =
 47 number of angles, (h, w) = dimension of the pictures. The first layer of the model conforms to n input
 48 channels (the number of slice projections) and 64 output channels with ReLU activation. 15 layers of
 49 Conv > batch normalization > ReLU with a consistent 64 channels follows and finally compressed
 50 into one channel at the last layer as the resulting image is produced. The kernel size is consistent at
 51 $(3, 3)$ and padding is set to preserve the original CT image resolution.

52 4 Initial Results

53 At the project's current state, we have successfully managed to perform training and produce some
 54 observable results in fig 5.

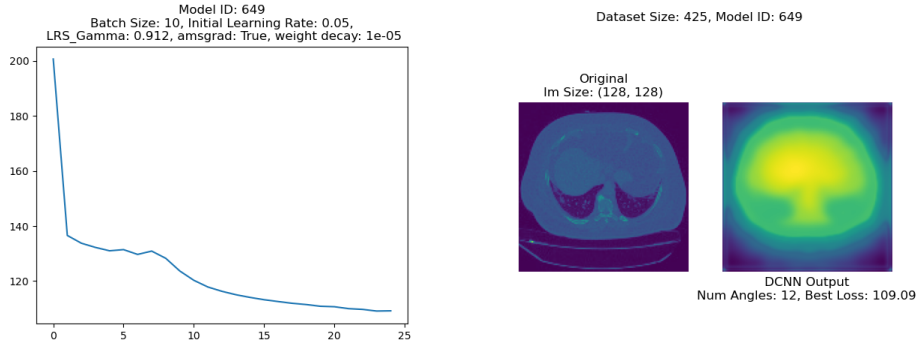


Figure 5: Initial Results

55 These results are without any hyperparameter tuning, model reconfigurations, or data preprocessing.
 56 One observation in the loss plot is we don't have validation testing set up yet.
 57 For reference, we are using a batch size of 10, learning rate $5e-2$, weight decay $1e-5$, and MSE
 58 loss. The optimizer is AMSGrad, which is an extension of the Adam Optimizer. We are also using
 59 ExponentialLR scheduler with $\gamma = .912$.

60 **5 Future Improvements**

61 **5.1 Improved Model/training**

62 We will consider changes to the model, however this might not be the forefront of our considerations
63 since [3] is a testament to the model’s optimality for our purpose. We will be looking more at the
64 hyperparameters such as learning rate, weight decay, batch size. We might consider other learning
65 rate schedulers aswell as a different optimizer, however the Adams optimizer is probably already
66 good enough.

67 **5.2 Improved Data Preprocessing**

68 An observation of our experimental results showcased a lack of confidence in our models recon-
69 struction of truth images. While the main culprit of this is likely due to dataset size, we theorize
70 that preprocessing methods may improve learning of our models. Therefore future dataset will
71 be preprocessed to improve contrast using methods such as Contrast Limited Adaptive Histogram
72 Equalization from the OpenCV library. By improving the contrast in truth images, we hope to imbue
73 our models with higher confidence for image reconstruction.

74 **References**

- 75 [1] Jonas Adler and Ozan Öktem. Learned primal-dual reconstruction. *IEEE Transactions on*
76 *Medical Imaging*, 37(6):1322–1332, 2018.
- 77 [2] Sayyed Mostafa Mostafavi. COVID19-CT-Dataset: An Open-Access Chest CT Image Repository
78 of 1000+ Patients with Confirmed COVID-19 Diagnosis, 2021.
- 79 [3] Dong Hye Ye, Gregery T. Buzzard, Max Ruby, and Charles A. Bouman. Deep back projection
80 for sparse-view ct reconstruction, 2018.